Repulsive bound-electron pairs in a Peierls lattice

U. A. Díaz-Reynoso, E. Huipe-Domratcheva and O. Navarro*

Unidad Morelia del Instituto de Investigaciones en Materiales, Universidad Nacional Autónoma de México,
Antigua Carretera a Pátzcuaro 8701, Colonia Ex Hacienda de San José de la Huerta, 58190 Morelia, Michoacán, México.
*e-mail: navarro@unam.mx

A new class of repulsive bound-electron pairs have been found in a Peierls lattice within the Hubbard model for energies $E < 0$ despite $U > 0$. These new repulsive bound-electron pairs have a high degree of localization as both the correlation energy U and the t_S/t_L hopping ratio increases. In order to study electronic correlation in Peierls lattices, our previous real space mapping method has also been extended to the so called generalized mapping method which is briefly presented here. In this paper, we concentrate our attention to discuss in detail the two-particle problem within a repulsive Hubbard model for the one-dimensional Peierls lattice.

1. Introduction

The recent experimental results by Winkler *et al.* [1] on the repulsive bound-atom pairs of ultracold rubidium atoms in an optical lattice, provides a new opportunity to study the pairing mechanism in its different forms. One of the first stable composite objects was the Cooper pair which gives the origin of the well known BCS theory of superconductivity [2]. It has been found that pairing exist also in the new high-Tc ceramic superconductors, and that in general these Cooper pairs could be between holes or between electrons, the composite Cooper pair of two attractive electron or two attractive holes is still fundamental in order to explain the mechanism of the high-T$_C$ superconductors [3]. Also, in the early 90′s the experimental demonstration of the Bose-Einstein condensation with ultracold atoms [4], provide an environment to continue the studies of the strong interaction regime in condensed matter both by experimental or theoretical techniques. Previously [5–7], a simple procedure to derive analytic expressions for the energy and the wave function of the two-bosons states in a one-dimensional periodic lattice within the Hubbard model was proposed. The existence of stable repulsive bound-atoms pairs in optical lattices [1, 8], induces the idea of bound-pair states like the repulsive bound-electron pairs. The issue we want to address in this paper is the novel repulsive bound-electron pair in a Peierls lattice, within the on-site Hubbard model and the generalized real space mapping method. An exact solution for the energy spectrum and the wave function of repulsive bound-electron pairs is given for the one-dimensional Peierls lattice in the framework of the repulsive Hubbard model.

One of the simplest model which consider the strong electronic interaction is the Hubbard model [9], this model include implicitly all kind of effects to obtain bound-electron states through the parameters of the Hamiltonian. The renewed interest in this model comes due to the fact that it contains the basic ideas to investigate the bound-pair states,

and the dynamics of electron or hole pairs who are believed to be fundamental to explain even unconventional superconductivity. In previous work [10–12], we have studied widely the two-particle problem in different lattices within the Hubbard model and the real space mapping method which allow us also to analyze electron pairing even in complex and non-periodic lattices like the one-dimensional Fibonacci lattice [13, 14]. To study the strong electronic correlation in a Peierls lattice the real space mapping method ought to be extended to the so-called generalized mapping method.

One of the advantages of the mapping method is that allows us to diagonalize exactly the Hubbard Hamiltonian of an infinite lattice, by mapping the interacting many-body problem onto a one-body tight-binding problem in a higher dimensional space. The strong two-electron interaction is well described using the single-band Hubbard Hamiltonian,

$$H = \sum_{<i,j>,\sigma} t_{i,j} c_{i,\sigma}^\dagger c_{j,\sigma} + U \sum_i n_{i,\uparrow} n_{i,\downarrow}, \qquad (1)$$

where $<i,j>$ denotes nearest neighbor sites, therefore $t_{i,j} = t_{i,i+1} = t_i$ and for a one-dimensional Peierls lattice it is an alternating sequence of t_S (short hopping) and t_L (large hopping), $c_{i,\sigma}^\dagger$ and $c_{j,\sigma}$ are the creation and annihilation operators respectively with spin $\sigma = \uparrow$ or $\downarrow$, $n_{i,\sigma} = c_{i,\sigma}^\dagger c_{i,\sigma}$ at site i, and U is the on-site Coulomb repulsion. Our paper is organized as follows, a discussion of the generalized mapping method will be presented in Sec. 2. Results and discussion for the repulsive two-electron pair in a Peierls lattice will be presented in Sec. 3. Some conclusions are given in Sec. 4.

2. Generalized mapping method

In the following, we introduce briefly the generalization of the mapping method for two electrons with opposite spin in an infinite periodic one-dimensional Peierls lattice. The two-electron states associated to this Peierls lattice within a Hubbard Hamiltonian form a square network of states with an
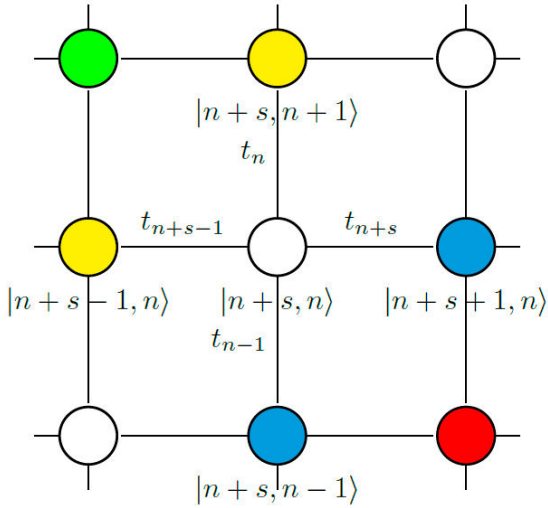
FIGURE 1. Diagram of neighbors states and hopping for a two electron state $|n + s, n\rangle$.

infinite number of impurities localized along the principal diagonal (see Fig. 1), which can be described with a type of tight-binding Hamiltonian. It is important to mention that sites in this new tight-binding Hamiltonian represent many-body states and not the atomic orbital or the Wannier functions commonly used. In Fig. 1, $n + s$ and n are the coordinates in this new space of states in order to be as general as possible.

Taking the definition of the two-electron wave function as $|i, j\rangle = |i \uparrow\rangle \otimes |j \downarrow\rangle$, we can obtain the relations associated with each hopping and site energy given in Fig. 1 as following: the Hubbard Hamiltonian applied to the above two particle wave function gives

$$H |n + s, n\rangle = t_{n+s} |n + s + 1, n\rangle + t_{n-1} |n + s, n - 1\rangle$$
$$+ t_{n+s-1} |n + s - 1, n\rangle + t_n |n + s, n + 1\rangle$$
$$+ U\delta_{0,s} |n + s, n\rangle, \tag{2}$$

therefore, the different site energies and the hopping terms can be obtained by

$$\langle n + s, n| H |n + s, n\rangle = U\delta_{0,s}, \tag{3}$$
$$\langle n + s + 1, n| H |n + s, n\rangle = t_{n+s}, \tag{4}$$
$$\langle n + s - 1, n| H |n + s, n\rangle = t_{n+s-1}, \tag{5}$$
$$\langle n + s, n - 1| H |n + s, n\rangle = t_{n-1}, \tag{6}$$
$$\langle n + s, n + 1| H |n + s, n\rangle = t_n. \tag{7}$$

To solve the square lattice of two-electron states (sites in Fig. 1), we have to diagonalize a matrix of the order of N^2 (N is the number of sites), that has a computational complexity of the order of $\mathcal{O}(N^6)$. Nevertheless, it can take advantage of the translational symmetry of the lattice on both, the impurities along the principal diagonal and the hopping, to project the square network of states onto a coupled of linear chains of effective states (see Fig. 2) in order to reduce its computational complexity to the order of $\mathcal{O}(N^4)$. This projection method resembles the used by Falicov and Yndurain in their work on the electronic structure of diamond [15]. The projection can be done by introducing a basis change given by:

$$|k; s\rangle = \frac{1}{\sqrt{N}} \sum_n e^{ikn} |n + s, n\rangle, \tag{8}$$

where $|k; s\rangle$ represent the new effective states (see Fig. 2) and $k \in \{0, (2\pi \cdot 1/N), (2\pi \cdot 2/N), \ldots, (2\pi \cdot (N-1)/N)\}$.

The matrix elements associated with the network of effective states (Fig. 2) are given by:

$$\langle l; s| H |k; s\rangle = \frac{1}{N} \left(\sum_m e^{-ilm} \langle m + s, m| \right)$$
$$\times H \left(\sum_n e^{ikn} |n + s, n\rangle \right)$$
$$= \frac{1}{N} \sum_m e^{-i(l-k)m} U\delta_{0,s} = U\delta_{l,k}\delta_{0,s}, \tag{9}$$
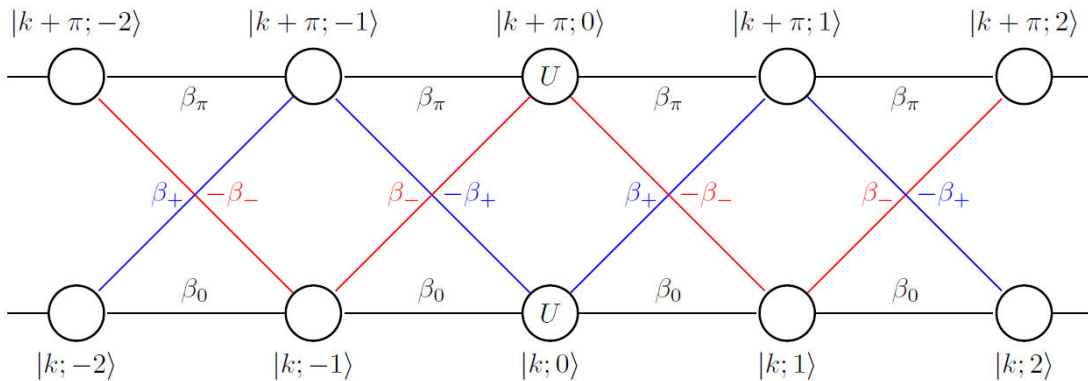

FIGURE 2. Equivalent structure representation of the network of states given in Fig. 1 after a basis change. Here, the sites represent effective states and the lines effective hopping, both are described in the text.

$$\langle l; s+1 | H | k; s \rangle = \frac{1}{N} \left(\sum_m e^{-ilm} \langle m+s+1, m | \right)$$

$$\times H \left(\sum_n e^{ikn} | n+s, n \rangle \right)$$

$$= \frac{1}{N} \sum_m e^{-ilm} \left(t_{m+s} e^{ikm} + t_m e^{ik(m+1)} \right)$$

$$= \left(e^{ik} + e^{i(l-k)s} \right) \frac{\tau(l-k)}{N}, \qquad (10)$$

where $\tau(k) = \sum_m e^{-ikm} t_m$ is the Fourier transform of t_m. Here, the following identities have been used:

$$\sum_m e^{-ilm} t_{m+s} e^{ikm} = e^{i(l-k)s} \sum_m e^{-i(l-k)(m+s)} t_{m+s}$$

$$= e^{i(l-k)s} \tau(l-k), \qquad (11)$$

$$\sum_m e^{-ilm} t_m e^{ik(m+1)} = e^{ik} \sum_m e^{-i(l-k)m} t_m$$

$$= e^{ik} \tau(l-k). \qquad (12)$$

The t_m sequence of the Peierls lattice, $t_S, t_L, t_S, t_L, \ldots$, has period 2, so, the only non-zero terms are $\tau(0)$ and $\tau(\pi)$:

$$\tau(0) = \sum_m e^{-i0m} t_m = \sum_m t_m = N \cdot \frac{t_S + t_L}{2}, \qquad (13)$$

$$\tau(\pi) = \sum_m e^{-i\pi m} t_m = \sum_m (-1)^m t_m = N \cdot \frac{t_S - t_L}{2}. \qquad (14)$$

In Fig. 2, every $|k; s\rangle$ is connected with $|k; s \pm 1\rangle$ and $|k + \pi; s \pm 1\rangle$. Therefore, each effective state has the site energies and the four adjacent effective hoppings given by the following relations:

$$\langle l; s | H | k; s \rangle = \delta_{0,s} \delta_{l,k} U, \qquad (15)$$

$$\langle k; s+1 | H | k; s \rangle = \left(e^{ik} + 1 \right) \frac{t_S + t_L}{2}, \qquad (16)$$

$$\langle k + \pi; s+1 | H | k; s \rangle = \left(e^{ik} + (-1)^s \right) \frac{t_S - t_L}{2}. \qquad (17)$$

The four different effective hopping integrals are named by:

$$\beta_0 = (e^{ik} + 1) \frac{t_S + t_L}{2}, \qquad (18)$$

$$\beta_\pi = (-e^{ik} + 1) \frac{t_S + t_L}{2}, \qquad (19)$$

$$\beta_+ = (e^{ik} + 1) \frac{t_S - t_L}{2}, \qquad (20)$$

$$\beta_- = (e^{ik} - 1) \frac{t_S - t_L}{2}. \qquad (21)$$

So, for each $k \in \{0, (2\pi \cdot 1/N), \ldots, (2\pi \cdot ([N/2] - 1)/N)\}$, we have a 2N-sites independent Hamiltonian to diagonalize

with a computational complexity of the order of $\mathcal{O}(N^3)$. Henceforth, we assume that $0 \leq k < \pi$.

In general, each eigenvector (ψ_k) can be written as:

$$\psi_k = \sum_s \left(a_{k,s} | k; s \rangle + a_{k+\pi,s} | k + \pi; s \rangle \right), \qquad (22)$$

where $a_{k,s}, a_{k+\pi,s} \in \mathbb{C}$ and s is the diagonal number. The wavefunction associated with the diagonal s can be expressed as $\psi_k(s) = a_{k,s} | k; s \rangle + a_{k+\pi,s} | k + \pi; s \rangle$ and its electronic contribution is $|\psi_k(s)|^2 = |a_{k,s}|^2 + |a_{k+\pi,s}|^2$. The same wavefunction in real space will be noted by $\psi_k(i, j)$.

3. Results and discussion

We will analyze briefly the behavior of the two-electron wave-functions in the Peierls lattice for the non-correlated ($U = 0$) and the correlated ($U \neq 0$) cases. The objective is to make clear the differences between them in the electronic structures.

3.1. Non-correlated two-electron wave-functions

For $U = 0$, the two-electron wave-function is the product of two one-electron wave-functions and its energy is the sum of two one-electron energies. Then, the two-electron density of states (DOS) is the convolution of two one-electron DOS. Taking a look of the valence and conduction band for the one-dimensional Peierls lattice, its easy to see that the one-electron energy at the valence band is $-2(|t_S| + |t_L|) \leq E \leq -2(|t_S| - |t_L|)$ while at the conduction band is $2|t_S - t_L| \leq E \leq 2|t_S + t_L|$, each band has $2|t_S|$ bandwidth. There are three different possibilities for the combinations of the two-electron wave-functions; a) two electrons in the valence band $-2(|t_S| + |t_L|) \leq E \leq -2(|t_S| - |t_L|)$, b) one electron in the valence band and one in the conduction band $-2|t_L| \leq E \leq 2|t_L|$, and c) two electrons in the conduction band $2(|t_S| - |t_L|) \leq E \leq 2(|t_S| + |t_L|)$. Depending on the t_S and t_L values, the DOS shows one full band with a $4|t_S + t_L|$ bandwidth or three small bands each one with $4|t_L|$ bandwidth.

3.2. Correlated two-electron wave-functions

In Fig. 3, the electronic density of states is shown for $U = 9$ and $t_S/t_L = 3$ (we will use $t_L = -1$ thorough this paper). It can be observed three big bands and three small ones. The big bands at the energy intervals [-8,-4], [-2,2] and [4,8] correspond to the non-correlated case (two electrons in the valence band, one electron in the valence band and one in the conduction band, or two electrons in the conduction band). The small two bands for energies $E > 8$ are the correlated bands, where each wave-function is a repulsive bounded-electron pair, the main electronic contribution is along the principal diagonal $s = 0$. Similar repulsive bound-pairs of atoms have been found experimentally and show that they can exist at milliseconds [1], they also were analyzed theoretically within
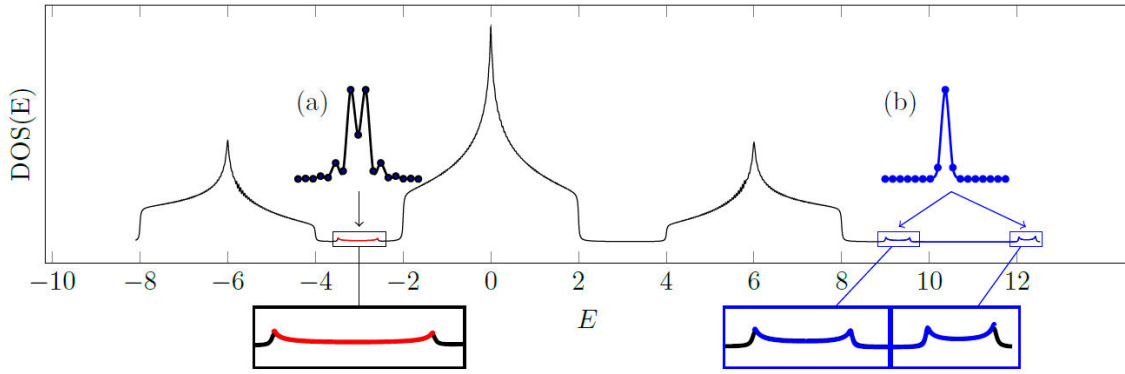
FIGURE 3. Density of states for $U = 9, t_L = -1, t_S/t_L = 3$. a) Band of two-electron states due to correlation with $E < 0$, they are mostly localized along the off diagonal in $s = \pm 1$. b) Band of two-electron states due to correlation with $E > 0$, they are mostly localized along the principal diagonal in $s = 0$.

the Hubbard model for bosons [8]. The energy associated to these states is very close to U. The correlation band between $-4 < E < -2$ for electrons has not been reported before, but similar results for bosons has been introduced in a early paper by Liberto *et al.* [7]. In this band, it is found that for each k there is a localized wave-function. In Fig. 4, the electronic contribution is shown along the diagonals $|\psi_k(s)|^2$ for each k. An exponential-decaying behavior is observed for all wave-functions, together with a maximum of the electronic density at $s = \pm 1$. A remarkable difference between this correlated band and the other two correlated band is that here, each wave-function has $E < 0$ despite the repulsion potential $U > 0$.

Figure 5 shows that the degree of localization of the wave-function is a function of both U and t_S/t_L, resulting in an increase of the localization as both U and t_S/t_L increases. Nevertheless, these localized states exist even for small values of U and t_S/t_L close to 1. So, the localized states exist even for small values of U and $t_S/t_L - 1$. The behavior of the wave-functions for the small correlated band between

$-4 < E < -2$ was tracked for the space parameters region $U \in [(1/10), 200]$ and $t_S/t_L \in [1, 20]$.

To describe the degree of localization of the wave-function, we have fitted the electronic contribution $|\psi_k(s)|^2$ to the function $|\psi_k(s)|^2 = Ae^{\lambda s}$, therefore, $\ln|\psi_k(s)|^2 = \ln A + \lambda s$. Here, λ is the parameter to quantify the degree of localization of the electronic density along the diagonals. Figure 6a) shows the value λ as function of U and t_S/t_L. Another important property that was calculated is the bandwidth of the small correlation band Δ_b, shown in Fig. 6b). The bandwidth shows a very similar behavior with λ, it tends to 2 as we move near the U and t_S/t_L axes and it decreases if both U and t_S/t_L increases. The energy of ψ_0 tend to 0 and the one of $\psi_{\pi/2}$ tend to 2 as we move near the U and t_S/t_L axes.

Finally, the band structure phase diagram describe 4 regions as it is shown in Fig. 6c). For the three cases (green,

FIGURE 5. Electron density $|\psi_0(i, j)|^2$ near the principal diagonal for a) $U = 0.1, t_S/t_L = 3.1$, b) $U = 8.1, t_S/t_L = 3.1$, c) $U = 0.1, t_S/t_L = 1.12$ and d) $U = 8.1, t_S/t_L = 1.12$. An increase in both U and t_S/t_L results in an increase in localization. Localized states exist even for small U and t_S/t_L near to 1.
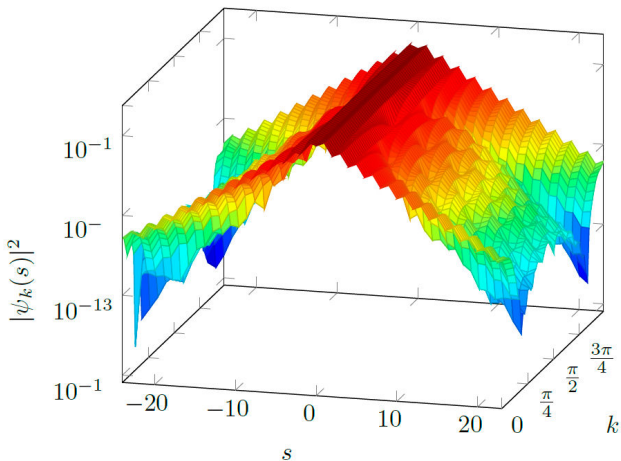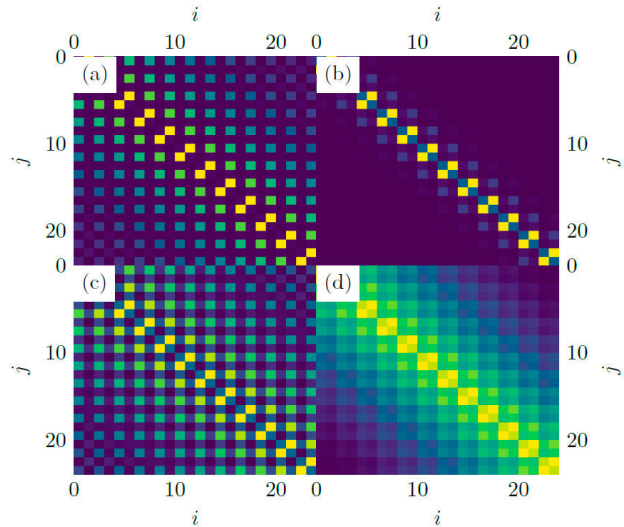

FIGURE 4. Electronic density distribution $|\psi_k(s)|^2$ for all states in the band. They tend to vanish exponentially outside the principal diagonal, thus all states are localized.
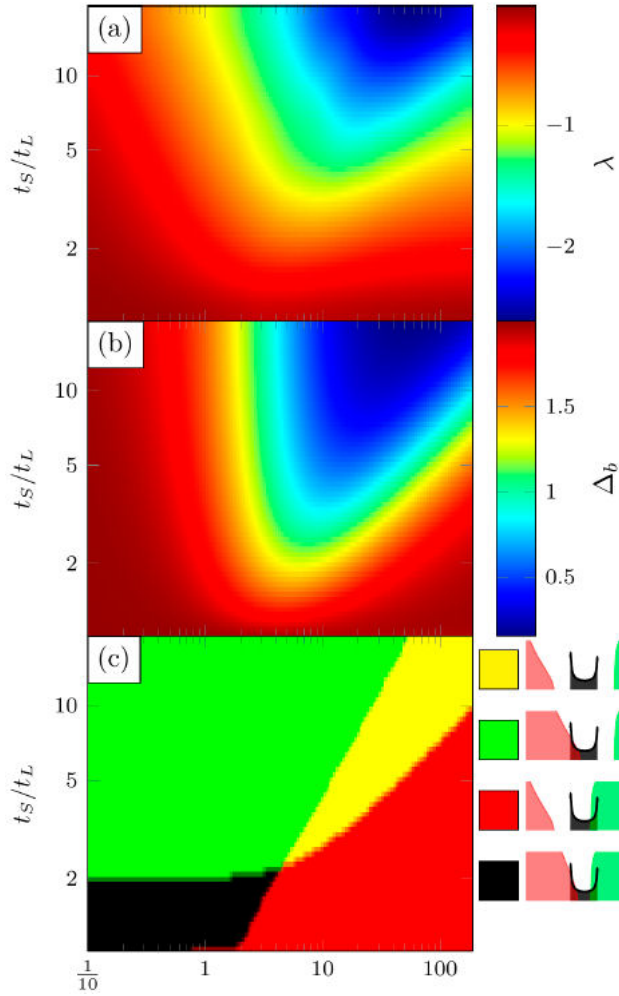
FIGURE 6. a) The decay parameter λ as function of U and t_S/t_L. b) The correlation bandwidth Δ_b as function of U and t_S/t_L. c) Different band structures as function of U and t_S/t_L. The correlation band can be: inside the two non-correlation bands (black), inside the first non-correlation band (green), touching the second non-correlation band (red) and between the first two non-correlation bands (yellow).

red and black), the small correlation band is almost hidden inside the non-correlation bands, where it is difficult for a material to show any different electronic properties from the usuals. In the fourth case (in yellow), the correlation band is between the two non-correlation bands and is the most interesting case. Here, the excited two-electron states appears and have lower energy than that of one-electron state in the valence band and the other in the conduction band, resulting in a lower band gap and in a higher conductivity compared to that expected for the one-electron treatment.

4. Conclusion

We have derived an exact solution of the novel repulsive bound-electron states in a one-dimensional Peierls lattice within the Hubbard model. The localization of these bound-electron states exist even for small values of the repulsive $U > 0$ Hubbard parameter and the t_S/t_L ratio very close to 1. The energy of the bound-electron pair is negative and is located between the energy of two electrons in the valence band and the energy of one electron in the valence band and other one in the conduction band. A generalization of the real space mapping method has also been introduced. Our results might be also relevant on the pairing mechanism of the high-T_C superconductors.

Acknowledgments

1. K. Winkler, G. Thalhammer, F. Lang, R. Grimm, J. Hecker Denschlag, A. Daley, A. Kantian, H.P. Buchler, and P. Zoller, *Repulsively bound atom pairs in an optical lattice*, Nature **441** (2006) 853.

2. J. Bardeen, L.N. Cooper, and J.R. Schrieffer, *Microscopic theory of superconductivity*, Phys. Rev. B **106** (1957) 162.

3. *The Physics of Superconductors*, Edited by K.H. Bennemann, and J.B. Ketterson (Springer, 2003).

4. A. Griffin, D.W. Snoke, and S. Stringari (editors), *Bose-Einstein Condensation* (Cambridge University Press, Cambridge, 1995).

5. M. Valiente, and D. Petrosyan, *Two-particles states in the Hubbard model*, J. Phys. B **41** (2008) 161002.

6. M. Valiente, and D. Petrosyan, *Scattering resonances and two-particle bound states of the extended Hubbard model*, J. Phys. B **42** (2009) 121001.

7. M. Di Liberto, A. Recati, I. Carusotto, and C. Menotti, *Two-body physics in the Su-Schrieffer-Heeger model*, Phys. Rev. A **94** (2016) 062704.

8. Y.-M. Wang, and J.-Q. Liang, *Repulsive bound-atoms pairs in an optical lattice with two-body interaction of nearest neighbors*, Phys. Rev. A **81** (2010) 045601.

9. J. Hubbard, *Electronic correlations in narrow energy bands*, Proc. Roy. Soc. (London) Ser. A **276** (1963) 238.

10. O. Navarro, and C. Wang, *Apareamiento electrónico en el hamiltoniano de Hubbard extendido*, Rev. Mex. Fis. **38** (1992) 553.

11. O. Navarro, and C. Wang, *An exact method to solve the diluted extended Hubbard model*, Solid State Commun. **83** (1992) 473.

12. L.A. Perez, O. Navarro, and C. Wang, *Nonperturbative results for attractive Hubbard pairing in triangular lattices*, Phys. Rev. B **53** (1996) 15389.

13. E. Vallejo, and O. Navarro, *Hubbard model in one dimension with a general bond charge interaction: Analytical ground-state solution for the pairing of two particles*, Phys. Rev. B **67** (2003) 193105.

14. E. Vallejo, and O. Navarro, *Analytical solution for pairing of two-particles in a quasiperiodic lattice within the Hubbard model*, J. Non-Cryst. Solids **329** (2003) 131.

15. L.M. Falicov and F. Yndurain, *Model calculation of the electronic structure of a (111) surface in a diamond-structure solid*, J. Phys. C **8** (1975) 147.